

Article

The Significance of Chimpanzee Occipital Asymmetry to Hominin Evolution

Shawn Hurst^{1,*}, Ralph Holloway², Alannah Pearson³ and Grace Bocko¹¹ Biology Department, University of Indianapolis, Indianapolis, IN 46227, USA; bockog@uindy.edu² Anthropology Department, Columbia University, New York, NY 10027, USA; rlh2@columbia.edu³ School of Archaeology and Anthropology, The Australian National University, Canberra 2601, Australia; alannah.pearson@anu.edu.au

* Correspondence: hursts@uindy.edu; Tel.: +1-317-788-4912

Abstract: Little is known about how occipital lobe asymmetry, width, and height interact to contribute to the operculum of the posterior parietal lobe, despite the utility of knowing this for understanding the relative reduction in the size of the occipital lobe and the increase in the size of the posterior parietal lobe during human brain evolution. Here, we use linear measurements taken on 3D virtual brain surfaces obtained from 83 chimpanzees to study these traits as they apply to operculum of the posterior occipital parietal arcus or bridging gyrus. Asymmetry in this bridging gyrus visibility provides a unique opportunity to study both the human ancestral and human equivalently normal condition in the same individual. Our results show that all three traits (occipital lobe asymmetry, width, and height) are related to this operculum and bridging gyrus visibility but width and not height is the best predictor, against expectations, suggesting that relative reduction of the occipital lobe and exposure of the posterior parietal is a complex phenomenon.

Keywords: chimpanzee; occipital; hominin

Citation: Hurst, S.; Holloway, R.; Pearson, A.; Bocko, G. The Significance of Chimpanzee Occipital Asymmetry to Hominin Evolution. *Symmetry* **2021**, *13*, 1862. <https://doi.org/10.3390/sym13101862>

Academic Editor: Antoine Balzeau

Received: 18 August 2021

Accepted: 29 September 2021

Published: 3 October 2021

Publisher's Note: MDPI stays neutral with regard to jurisdictional claims in published maps and institutional affiliations.



Copyright: © 2021 by the authors. Licensee MDPI, Basel, Switzerland. This article is an open access article distributed under the terms and conditions of the Creative Commons Attribution (CC BY) license (<https://creativecommons.org/licenses/by/4.0/>).

1. Introduction

In addition to helping us understand the evolution of lateralization [1–3], asymmetries of the brain's surface seen in closely related species such as chimpanzees (*Pan troglodytes*) can also help us to understand the role development plays in brain evolution itself. As an example, a major shape difference in the brains of human (*Homo sapiens*) versus nonhuman primates is that in nonhuman primates the occipital lobe operculates part of the parietal lobe, including a buried annectant gyrus that connects these lobes, known as the 1st parieto-occipital “pli de passage” of Gratiolet or the parieto-occipital arcus [4–6]. The posterior portion or bridge of this gyrus is consistently seen on the brain's surface in humans but is only occasionally seen (often asymmetrically) in chimpanzees [4–8]. Relative reduction of the occipital operculum and expansion of the posterior parietal lobe is a major hallmark in human brain evolution, although debate on when this occurred has been contentious, and currently we have no model of what transitional states between the human ancestral and derived conditions may have looked like. Studying the presence or absence of a visible bridging gyrus in chimpanzees, who are our closest living relatives and who have brains very similar to that of the last common ancestor [7–10] allows us to understand its relationship to the size of the occipital lobe; when this trait is asymmetrical in chimpanzees (who unlike humans still show occasional asymmetry in this region) it allows us to understand this trait developmentally rather than genetically, as it occurs variably in different hemispheres of the same individual, while giving us a greater range of variation in which to build models of transitional states, and to study the evolution of asymmetries and symmetries, since it is asymmetrical in chimpanzees while it is symmetrical in humans. Such an understanding would also be very valuable for the interpretation of hominin endocranial casts, which have morphology that is difficult to interpret in this region due to

our lack of transitional models, and so very valuable to the study of brain evolution. If this trait is only associated with occipital lobe height this would suggest that the primary factor in the exposure of the bridging gyrus is posterior movement of the occipital operculum, which retracted inferio-posteriorly during human evolution revealing buried parietal gyri which then expanded; association with asymmetry and/or width in addition to height would suggest a relative change in the size and shape of the entire occipital to the parietal lobe is a more important factor. Using preliminary data, we observed these relationships in a large sample of chimpanzees. The aim of this study is an exploratory assessment of whether the presence or absence of the occipital bridging gyrus is associated with left or right hemispheres, and how hemisphere siding is associated with occipital lobe width and height in the chimpanzee brain. Regression analysis examines the correlation between left and right hemispheres and occipital lobe width and height, where reliable predictions (± 1 s.e.) determined if occipital lobe height or width was a more reliable predictor of hemisphere siding. Ultimately, we found that asymmetry, height, and width are all associated with a visible bridging gyrus, in increasing order.

2. Materials and Methods

This study used three-dimensional surface models of a sample of 83 chimpanzee brains. These brains were reconstructed using MRIs from the National Chimpanzee Brain Resource (<https://www.chimpanzeebrain.org> (accessed on 1 September 2021)) using BrainVISA software (Pune, India) and measured using MeshLab [11–13]. Although the measurements were able to be collected on the entire sample, the original collectors [12] could not guarantee that the left or right hemisphere siding was correctly labelled. To accommodate this uncertainty, subsample ($n = 15$) was obtained by one of us to allow a comparison and analysis of ‘known’ and ‘unknown’ hemisphere siding’. Each brain was rotated such that the lowest points of the left occipital and left temporal lobes both lie on a plane at right angles to the longitudinal fissure. The width of each hemispherical occipital lobe was measured as the distance in millimeters from the longitudinal fissure to the lobe’s most lateral extent. Height was measured as the greatest vertical extent between points on each hemispherical lobe, barring its most medial edge if a bridging gyrus was visible; the presence of a visible bridging gyrus between the superior-medial occipital lobe and the parietal-occipital arcus was scored as a Y, while a fully operculated and thus hidden bridging gyrus was scored as an N (see Figure 1).

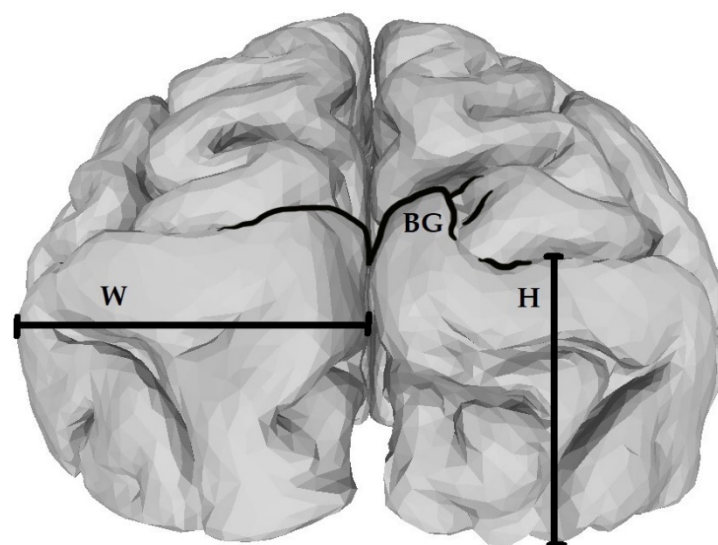


Figure 1. Occipital Measurement Definitions. W = width, H = height. The right hemisphere has a bridging gyrus (BG) not fully operculated by the occipital lobe and was scored as a Y; in the left hemisphere this gyrus is fully operculated, so its condition was scored as an N.

Statistical Analyzes

Preliminary analysis included a measurement error study. All data collection and measurements were conducted by a single operator to prevent the effects on interobserver error. Measurement error was investigated by using an analysis of variance, where measurement error was calculated as the proportion of the mean-squared differences between replicates relative to the total between-group variation [14]. The subsample ($n = 15$) of known hemisphere siding were measured on two separate occasions and measurement error (ME) calculated as $\% ME = 100 \times MS(\text{within}) / MS(\text{within}) + MS(\text{among})$. Measurement error ranged from 0% to 3% (results not shown), and with this low measurement error, we considered intraobserver error had a very minimal effect on further analyzes.

Canonical Correspondence Analysis (CCA) initially examined the potential association between the four metrics: occipital height, both left and right (in mm) and width, both left and right (in mm), and the presence or absence of a left, right, or no occipital bridge (Table 1). CCA is particularly suited to datasets where quantitative variables and presence/absence variables are common, such as ecological datasets [15]. Only recently has this been applied to brain evolution, specifically quantitative variables, and the presence/absence of sulcal patterns [16]. CCA allows a comparison analysis, directly testing a priori hypotheses emphasizing the variance of Y that is related to X , and where CCA combines the properties of both ordination and regression analyses to produce ordinations of Y that are linearly constrained to X [15]. Correlation analysis then tested the strength of the potential correlation between two or more variables using the most common correlation statistic (Pearson's r correlation coefficient), with a two-tailed significance that the variables were uncorrelated and a Monte Carlo permutation (using 9999 iterations) [17].

Table 1. Occipital lobe measurements and bridging pattern type.

Subject	Height ¹		Width		Bridge ²		
	L	R	L	R	L	R	Both
Abby	36	38	38	37	N	N	N
Agatha	42	44	47	46	N	N	N
Ahni	28	31	35	36	N	N	N
Akimel	42	41	39	41	N	N	N
Alex *	26	27	34	34	Y	Y	Y
Alpha	33	35	36	39	N	N	N
Amanda	41	41	37	37	N	N	N
Angie	27	30	35	35	Y	N	N
Artemus	32	33	35	35	N	Y	N
Arthur	38	37	33	35	N	N	N
Artifee *	39	37	37	36	N	N	N
Augusta	38	35	32	34	N	N	N
Azalea	36	38	33	37	N	N	N
Bahn	35	36	33	33	N	N	N
Barbara	42	43	37	37	N	N	N
Bart	31	29	37	37	N	Y	N
Bashful *	31	32	34	34	N	N	N
Becca	36	38	28	30	N	N	N
Beleka	32	31	28	30	N	N	N
Bernadette	35	39	32	36	N	N	N
Bernie	24	26	27	26	N	N	N
Beta	29	29	29	29	N	N	N
Betty *	44	44	36	38	N	N	N
Billy *	33	39	31	33	N	N	N
Bo *	35	33	33	33	N	N	N
Boka	42	42	38	37	Y	Y	Y
Brandy	35	34	26	29	N	N	N
Bria	34	38	38	40	Y	Y	Y
Brodie	33	33	31	31	N	N	N

Table 1. Cont.

Subject	Height ¹		Width		Bridge ²		
	L	R	L	R	L	R	Both
Callie	40	40	32	32	N	N	N
Carl *	37	32	33	34	Y	Y	Y
Chechkel	43	42	38	41	N	N	N
Cheeta *	45	44	37	39	N	N	N
Cheopi	34	34	31	32	N	N	N
Chester	28	36	37	37	Y	Y	Y
Chinook	35	38	36	36	N	N	N
Chip *	33	34	36	36	Y	Y	Y
Christa	43	43	34	37	N	N	N
Chuhia	37	40	34	34	N	Y	N
Cissie	38	41	35	37	N	N	N
Coco	31	32	37	38	Y	Y	Y
Cybil	27	28	33	34	Y	Y	Y
Dara	36	39	36	34	N	N	N
David *	29	29	37	35	N	Y	N
Drew	37	36	37	40	N	Y	N
Duff	39	39	35	37	N	N	N
Edwina *	31	32	32	32	N	N	N
Eesha	30	32	33	33	N	N	N
Ehsto	42	44	45	45	N	N	N
Elvira	39	39	38	37	Y	Y	Y
Elwood *	39	40	35	35	N	N	N
Emily *	30	32	35	35	N	N	N
Eniga	39	40	35	35	N	N	N
Evelyne	32	29	29	29	N	N	N
Faye	37	38	35	38	N	N	N
Fiona	38	41	38	37	N	N	N
Foxy	37	36	35	35	N	N	N
Frannie	34	35	34	34	N	N	N
Fritz	38	40	34	36	N	N	N
Gaygos	36	35	39	39	N	N	N
Gelb	37	38	31	33	N	N	N
Gigi	34	33	35	35	N	N	N
Gimp	32	33	36	35	Y	N	N
Gisoki	38	40	30	35	N	N	N
Haakid	36	37	38	41	N	N	N
Hannah	35	35	32	33	N	N	N
Helga	30	27	33	35	Y	Y	Y
Heppie	42	42	36	37	N	N	N
Hobbes	30	36	33	32	Y	N	N
Hodari	36	36	37	37	N	N	N
Huey	37	29	37	38	N	Y	N
Hug	31	36	36	36	N	N	N
Huhkalig	38	38	35	36	N	N	N
Iyk	31	35	33	35	N	N	N
Jacqueline	33	31	34	34	N	Y	N
Jadyh	31	33	33	34	N	N	N
Jake	38	40	36	37	N	N	N
Jamie	38	37	37	38	N	N	N
Jane	33	32	38	37	N	N	N
Jarred *	32	33	33	33	N	N	N
Jcarter	35	31	32	34	N	Y	N
Jewelle	28	27	30	29	Y	Y	Y
Jolson *	38	38	39	38	N	N	N

¹ All numbered measurements in left (L) and right (R) height and width in mm. ² Presence (Y), absence (N), or Both (B) of a visible bridging gyrus. * Indicates the subsample of individuals with known siding.

To estimate the uncertainty due to unknown hemisphere siding, a subsample ($n = 15$) where the hemisphere siding was known (left and right) was examined with Bivariate ordinary least-squares (OLS) regression to test the strength of association between each of the four variables and occipital lobe side (left and right hemisphere). For regression purposes, and to linearize scaling relationships [18], each variable was converted (from mm) into natural logarithmic units (base e) and a 95% confidence interval fitted to the log–log regressions.

Predicted height and width from both hemispheres was calculated using prediction equations provided by the bivariate OLS regression models, where $y = (a \times \log[x] + b)$. The reliability of the predictions was calculated as the percentage of prediction errors (PPE), where $PPE = (\text{predicted} - \text{observed})/\text{predicted} \times 100$. PPE calculates the uncertainty in an estimate relative to its size [19]. Prediction reliability was determined by applying a bracket of uncertainty produced by the standard error (s.e.) from the bivariate OLS regression models calculating the upper and lower estimates for predicted height or width for each specimen relative to its size, where $y = (a \times \log[x] + b \pm \text{s.e.})$. This maintained any inherent differences between each variable allowing for changes in the range of uncertainty, where each variable is associated with differences in the standard error [20]. All statistical analyses were conducted in *Past 4.0* [21].

3. Results

Preliminary results from summary statistics (Table 2) detailing the differences between the left and right occipital lobes and the variation between height and width measurements.

Table 2. Summary statistics detailing mean, variance, standard deviations for the subsample ($n = 15$) with known hemisphere siding.

Summary Statistics (Known Sample)				
	L Height	R Height	L Width	R Width
N	15	15	15	15
Min	26	27	31	32
Max	45	44	39	39
Sum	522	526	522	525
Mean	34.8	35.06667	34.8	35
Std. error	1.40814	1.31	0.57	0.53
Variance	29.74286	25.78095	4.885714	4.285714
Stand. dev	5.453701	5.077495	2.210365	2.070197
Median	33	33	35	35
25 percentile	31	32	33	33
75 percentile	39	39	37	36
Skewness	0.4577742	0.476494	0.108067	0.613097
Kurtosis	−0.4279719	−0.52249	−0.60243	−0.46667
Geom. mean	34.40985	34.73166	34.73453	34.94389
Coeff. var	15.67156	14.47955	6.351624	5.914848

Canonical Correspondence Analysis (CCA) was used to determine the strength of the correlation between different occipital bridge types, and the left (L) and right (R) height or width of the occipital lobe. The presence or absence of bridging patterns requires assessment where the potential correlation between occipital lobe height and width could be assessed against the presence or absence of Left or Right bridging patterns, or whether those with Both patterns were associated more with Occipital lobe width or height. Consistent

with CCA, the type of bridging patterns grouped specimens accordingly and the effect of occipital lobe height or width determined. Results indicated that greater occipital width was associated with both Left and Right bridging patterns (Axis 1), while occipital lobe height (Axis 2) was associated more strongly with No Bridging pattern. The correlations between variables indicated by Axis 1 (89% variance) and Axis 2 (11% variance) were statistically significant ($p < 0.002$) with 1000 permutations (Table 3).

Table 3. Canonical Correspondence Analysis values of occipital lobe bridge patterns, with permutation (999 iterations). Statistically significant values are reported in italics.

Axis	Eigenvalue	Percentage	<i>p</i> -Value
1	0.2851	89.14	<i>0.001</i>
2	0.0347	10.86	<i>0.002</i>

Abbreviations: *p*-value is the permuted *p*-value from 1000 iterations.

There were four distinct groups based on the type of bridge patterns observed with a left bridge associated with marginally shorter L lobe height and greater R lobe width, a right bridge was associated with shorter R lobe height and slightly greater R lobe width, where both L and R bridges were present, these were weakly associated with smaller L height, and no bridges was associated with greater R lobe height and width (Figure 2).

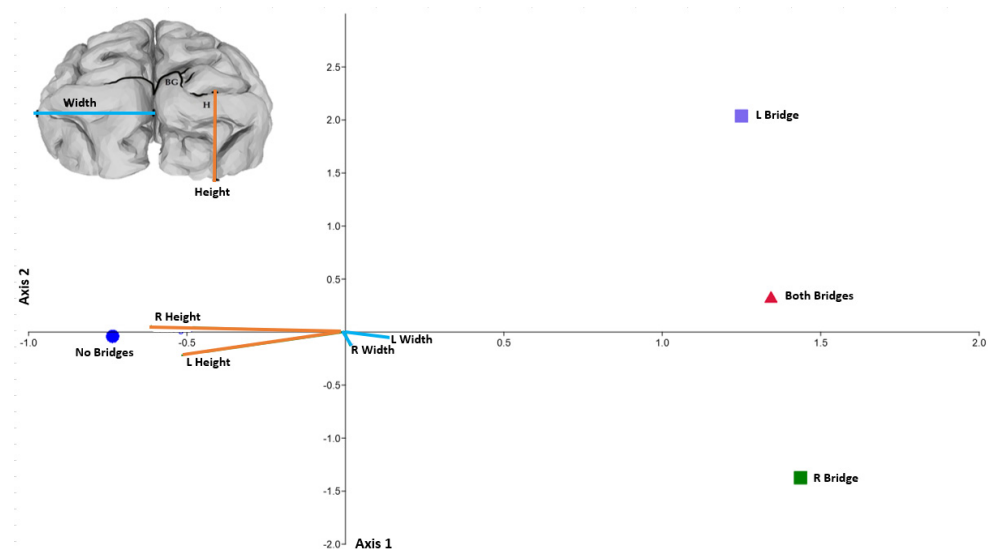


Figure 2. Canonical Correspondence analysis showing the four distinct groups of bridge patterns and a biplot indicating the direction of correlations between variables where longer lines indicate a stronger correlation. Abbreviations: Green square = Right Bridge; Purple square = Left bridge; Blue Sphere = No bridge; Red Triangle = Both bridges; L Height = Left occipital lobe height; R Height = Right occipital lobe height; L Width = Left occipital lobe width; R Width = Right occipital lobe width.

Correlation analysis examined potential correlations between variables using Pearson's r correlation coefficient for significance and a Monte Carlo permutation (9999 iterations) with the probability of variables being uncorrelated using a two-tailed significance set to $p < 0.01$. Statistically significant correlations using Monte Carlo permutation are reported (Table 4) for R and L lobe height and width ($p \leq 0.0001$), with slightly less robust correlations for R lobe width and right bridge ($p = 0.0008$), and L lobe height and L bridge ($p = 0.0022$). Correlations between bridging patterns are entirely due to the binary coding and do not reflect a true correlation.

Table 4. Correlation Analysis between occipital lobe metrics and bridging patterns, with Monte Carlo permutation (9999 iterations) and two-tailed significance. Statistically significant values are reported in italics ($p < 0.01$). Correlation values reported in the lower triangle with two-tailed significance that variables are uncorrelated are reported in the upper triangle.

Correlation Table							
	L Height	R Height	L Width	R Width	L Bridge ¹	R Bridge ¹	N Bridge ¹
L Height		0.0001	0.0001	0.0001	0.0022	0.0161	0.0026
R Height	<i>0.0001</i>		0.0001	0.0001	0.0101	0.0008	0.0002
L Width	<i>0.0001</i>	<i>0.0001</i>		0.0001	0.6361	0.3920	0.4240
R Width	<i>0.0001</i>	<i>0.0001</i>	<i>0.0001</i>		0.8226	0.7199	0.9431
L Bridge	<i>0.0022</i>	<i>0.0101</i>	0.6361	0.8226		0.0001	0.0001
R Bridge	<i>0.0161</i>	<i>0.0008</i>	0.3920	0.7199	0.0001		0.0001
N Bridge	<i>0.0026</i>	<i>0.0002</i>	0.4240	0.9431	0.0001	0.0001	

Abbreviations: Correlation in lower triangle of matrix; probability of uncorrelated variables with two-tailed significance ($p < 0.05$) in upper triangle of matrix. L Height = Left occipital lobe height; R Height = Right occipital lobe height; L Width = Left occipital lobe width; R Width = Right occipital lobe width; R Bridge = Right Bridge; L Bridge = Left bridge; No Bridge = Nbridge; ¹ = Included as binary values (present/absent scores).

Caution is warranted with these initial findings where uncertainty associated with correct hemisphere siding, and the low number of individuals who possessed a bridging pattern could be obscured by the higher number of those who possessed no bridging pattern and where known siding is uncertain. However, correlation results and those reported from the CCA suggest a likely association between lobe width and bridging patterns.

Ordinary Least Squares (OLS) regression examined a subsample ($n = 15$) of individuals with known right and left hemisphere siding allowing a test of bridging and siding prediction and associated uncertainty. Metrics (in mm) for both right and left width and height were first transformed by natural logarithm (base e) maintaining linearity. Both height and width were predicted using Right from Left and then Left from Right to determine the potential effect of siding on prediction uncertainty. All predictions were made with a 95% confidence interval (CI) with strong correlations ($r \geq 0.86$, $p \leq 0.0001$). However, between the regression models, there was little observable difference whether the left or right hemisphere was used for the predictions (Table 5, Figure 3).

Table 5. Parameters for ordinary least-squares regression detailing the regression statistics for the four metrics both left and right side. Statistically significant results reported in italics.

Right Lobe Regression Statistics					
Metrics	<i>a</i>	<i>b</i>	s.e	<i>r</i>	<i>p</i>
R Height	0.82901	0.61434	0.11182	0.90	<i>0.0001</i>
R Width	0.79421	0.73609	0.12819	0.86	<i>0.0001</i>
Left Lobe Regression Statistics					
Metrics	<i>a</i>	<i>b</i>	s.e	<i>r</i>	<i>p</i>
L Height	0.97553	0.07749	0.13158	0.90	<i>0.0001</i>
L Width	0.94058	0.20515	0.15181	0.86	<i>0.0001</i>

Abbreviations: *a* = slope; *b* = intercept; s.e = standard error of the regression estimate; *r* = Correlation coefficient; *p* = *p*-value for significance; L Height = Left occipital lobe height; R Height = Right occipital lobe height; L Width = Left occipital lobe width; R Width = Right occipital lobe width.

All regression models showed a strong prediction overall, calculating the percentage of prediction uncertainty (PPE) allows a better comparison of the uncertainty within each model. Percentage of prediction error (PPE) was calculated for occipital height and width, respectively, and the difference between these left and right predictions compared with robust agreement between the observed and the predicted values (Table 5). Prediction reliability assessed the difference within the regression models and between left and right

lobes. Greater prediction uncertainty existed for lobe height, with a disparity of 17%, than for width where the disparity was only 6%. This suggests that occipital lobe width might be a more stable variable with less prediction uncertainty than height, potentially making it more suitable for predicting occipital lobe side and hence, more reliable for assessing bridging pattern associations (Table 6).

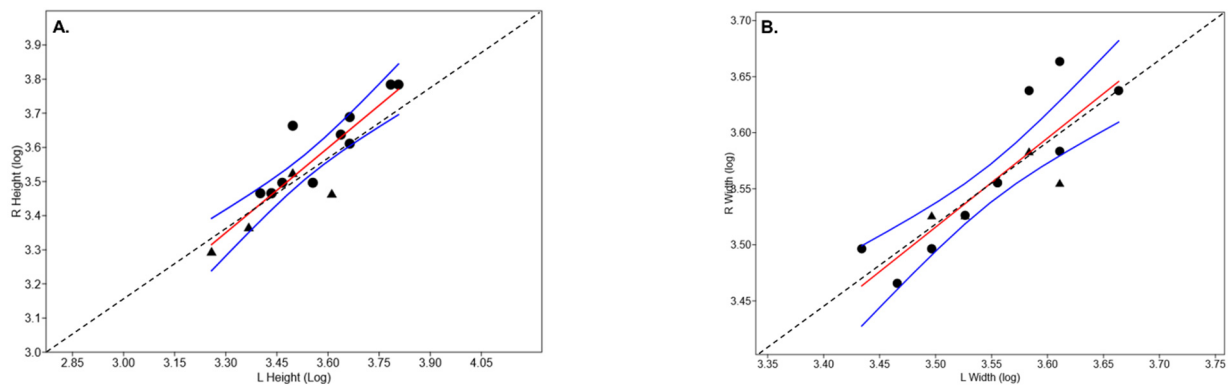


Figure 3. Log-log Ordinary Least Squares (OLS) regression of Occipital lobe fitted with a 95% confidence interval for lobe (A) height and (B) width where black triangles are specimens with a bridging gyrus and black dashed line to emphasize symmetry and asymmetry (the departure from symmetry).

The predictions for both L and R occipital lobe width and height are provided for both known and unknown sample, with predicted values converted from log-units to metrics (in mm) by taking the inverse-log and the observed values reported in parentheses alongside the predicted values (Table 7, Figure 4). Considering there was no discernible difference in pattern of reliability between the hemispheres, only the prediction of R lobe height and width are provided.

Table 6. Percentage of prediction errors (PPE) for four occipital metrics calculated as the difference between observed and predicted height and width, and percentage of prediction reliability calculated as difference between observed and predicted height and width (in mm) divided by observed height and width. Negative and positive values indicate an increase or decrease, respectively, in the predicted value from the observed.

Subject	Percentage Prediction Error			
	Height		Width	
	L	R	L	R
Alex	1%	1%	0%	0%
Artifee	−2%	1%	−1%	1%
Bashful	1%	0%	0%	0%
Betty	0%	−1%	1%	−2%
Billy	4%	−4%	2%	−1%
Bo	−2%	2%	0%	0%
Carl	−4%	4%	1%	0%
Cheeta	−1%	0%	1%	−2%
Chip	1%	0%	0%	0%
David	0%	1%	−2%	1%
Edwina	1%	0%	0%	1%
Elwood	0%	−1%	0%	0%
Emily	2%	−1%	0%	0%
Jarred	1%	0%	0%	0%
Jolson	0%	0%	−1%	0%

Table 6. Cont.

Reliability of Prediction Errors		
Subject	Height	Width
Alex	0%	0%
Artifee	3%	2%
Bashful	−1%	0%
Betty	0%	−3%
Billy	−9%	−3%
Bo	4%	1%
Carl	8%	−1%
Cheeta	1%	−3%
Chip	−1%	0%
David	1%	3%
Edwina	−1%	1%
Elwood	−1%	0%
Emily	−3%	0%
Jarred	−1%	1%
Jolson	0%	1%

Table 7. Prediction of occipital lobe width and height (in mm) listed with the corresponding variable calculated from the bivariate ordinary least-squares equations. Observed values reported beside predicted in parentheses.

Prediction of Height and Width				
Subject	Height ¹		Width ¹	
	R	L	R	L
Alex ²	28 (27)	26 (26)	34 (34)	34 (34)
Artifee ²	37 (37)	39 (39)	36 (36)	37 (37)
Bashful ²	33 (32)	31 (31)	34 (34)	34 (34)
Betty ²	43 (44)	43 (44)	38 (38)	36 (36)
Billy ²	39 (39)	33 (34)	34 (33)	31 (31)
Bo ²	34 (33)	35 (35)	34 (33)	33 (33)
Carl ²	33 (32)	37 (37)	34 (34)	33 (33)
Cheeta ²	43 (44)	44 (45)	38 (39)	37 (37)
Chip ²	34 (34)	33 (33)	36 (36)	36 (36)
David ²	30 (29)	29 (29)	35 (35)	37 (37)
Edwina ²	33 (32)	31 (31)	33 (32)	32 (32)
Elwood ²	39 (40)	39 (39)	35 (35)	35 (35)
Emily ²	33 (32)	30 (30)	35 (35)	35 (35)
Jarred ²	34 (33)	32 (32)	34 (33)	33 (33)
Jolson ²	38 (38)	38 (38)	38 (39)	39 (38)
Abby	38 (38)	36 (36)	37 (37)	38 (39)
Agatha	43 (44)	41 (42)	44 (46)	46 (47)
Ahni	32 (31)	28 (28)	36 (36)	35 (35)
Akimel	40 (41)	41 (42)	40 (41)	39 (39)
Alpha	35 (35)	33 (33)	38 (39)	36 (36)
Amanda	40 (41)	40 (41)	37 (37)	37 (37)
Angie	31 (30)	27 (27)	35 (35)	35 (35)
Artemus	34 (33)	32 (32)	35 (35)	35 (35)
Arthur	37 (38)	38 (37)	35 (35)	33 (33)
Augusta	35 (35)	38 (38)	34 (34)	32 (32)
Azalea	38 (38)	36 (36)	37 (37)	33 (33)
Bahn	36 (36)	35 (35)	34 (33)	33 (33)
Barbara	42 (43)	41 (42)	37 (37)	37 (37)
Bart	30 (29)	31 (31)	37 (37)	37 (37)
Becca	38 (38)	36 (36)	31 (30)	28 (28)

Table 7. Cont.

Subject	Prediction of Height and Width			
	Height ¹		Width ¹	
	R	L	R	L
Beleka	32 (31)	32 (31)	31 (30)	28 (28)
Bernadette	39 (39)	35 (35)	36 (36)	32 (32)
Bernie	28 (26)	24 (24)	28 (27)	27 (26)
Beta	30 (29)	29 (29)	30 (29)	29 (29)
Boka	41 (42)	41 (42)	37 (37)	38 (38)
Brandy	34 (34)	35 (35)	30 (29)	26 (26)
Bria	38 (38)	34 (34)	39 (40)	38 (39)
Brodie	34 (33)	33 (33)	32 (31)	31 (31)
Callie	39 (40)	39 (40)	33 (32)	32 (32)
Chechkel	41 (42)	42 (43)	40 (41)	38 (38)
Cheopi	34 (34)	34 (34)	33 (32)	31 (31)
Chester	36 (36)	28 (28)	37 (37)	37 (37)
Chinook	38 (38)	35 (25)	36 (37)	36 (37)
Christa	42 (43)	42 (43)	37 (37)	34 (34)
Chuhia	39 (40)	37 (37)	34 (34)	34 (34)
Cissie	40 (41)	38 (38)	37 (37)	35 (35)
Coco	33 (32)	31 (31)	38 (38)	37 (37)
Cybil	29 (28)	27 (27)	34 (34)	33 (33)
Dara	39 (39)	36 (36)	34 (34)	36 (36)
Drew	36 (36)	37 (37)	39 (40)	37 (37)
Duff	39 (39)	39 (39)	37 (37)	35 (35)
Eesha	33 (32)	30 (30)	34 (33)	33 (33)
Ehsto	43 (44)	41 (42)	43 (45)	44 (45)
Elvira	39 (39)	39 (39)	37 (37)	38 (38)
Eniga	39 (40)	39 (39)	35 (35)	35 (35)
Evelyne	30 (29)	32 (32)	30 (29)	29 (29)
Faye	38 (38)	37 (37)	38 (38)	35 (35)
Fiona	40 (41)	38 (38)	37 (37)	38 (38)
Foxy	36 (36)	37 (37)	35 (35)	35 (35)
Frannie	35 (35)	34 (34)	34 (34)	34 (34)
Fritz	39 (40)	38 (38)	36 (36)	34 (34)
Gaygos	35 (35)	36 (36)	38 (39)	39 (39)
Gelb	38 (38)	37 (37)	34 (33)	31 (31)
Gigi	34 (33)	34 (34)	35 (35)	35 (35)
Gimp	34 (33)	32 (32)	35 (35)	36 (36)
Gisoki	39 (40)	38 (39)	35 (35)	30 (30)
Haakid	37 (37)	36 (36)	40 (41)	38 (38)
Hannah	35 (35)	35 (35)	34 (33)	32 (32)
Helga	28 (27)	30 (30)	35 (35)	33 (33)
Heppie	41 (42)	41 (42)	37 (37)	36 (36)
Hobbes	36 (36)	30 (30)	33 (32)	33 (33)
Hodari	36 (36)	36 (36)	37 (37)	37 (37)
Huey	30 (29)	37 (37)	38 (38)	37 (37)
Hug	36 (36)	31 (31)	36 (36)	36 (36)
Huhkalig	38 (38)	38 (38)	36 (36)	35 (35)
Iyk	35 (35)	31 (31)	35 (35)	33 (33)
Jacqueline	32 (31)	33 (33)	34 (34)	34 (34)
Jadyh	34 (33)	31 (31)	34 (34)	33 (34)
Jake	39 (40)	38 (38)	37 (36)	36 (37)
Jamie	37 (37)	38 (38)	38 (38)	37 (37)
Jane	33 (32)	33 (33)	37 (38)	38 (37)
Jcarter	32 (31)	35 (35)	34 (34)	32 (32)
Jewelle	28 (27)	28 (28)	30 (29)	30 (30)

Abbreviations: ¹ Measurements of left (L) and right (R) height and width (in mm), ² The subsample with known hemisphere siding.

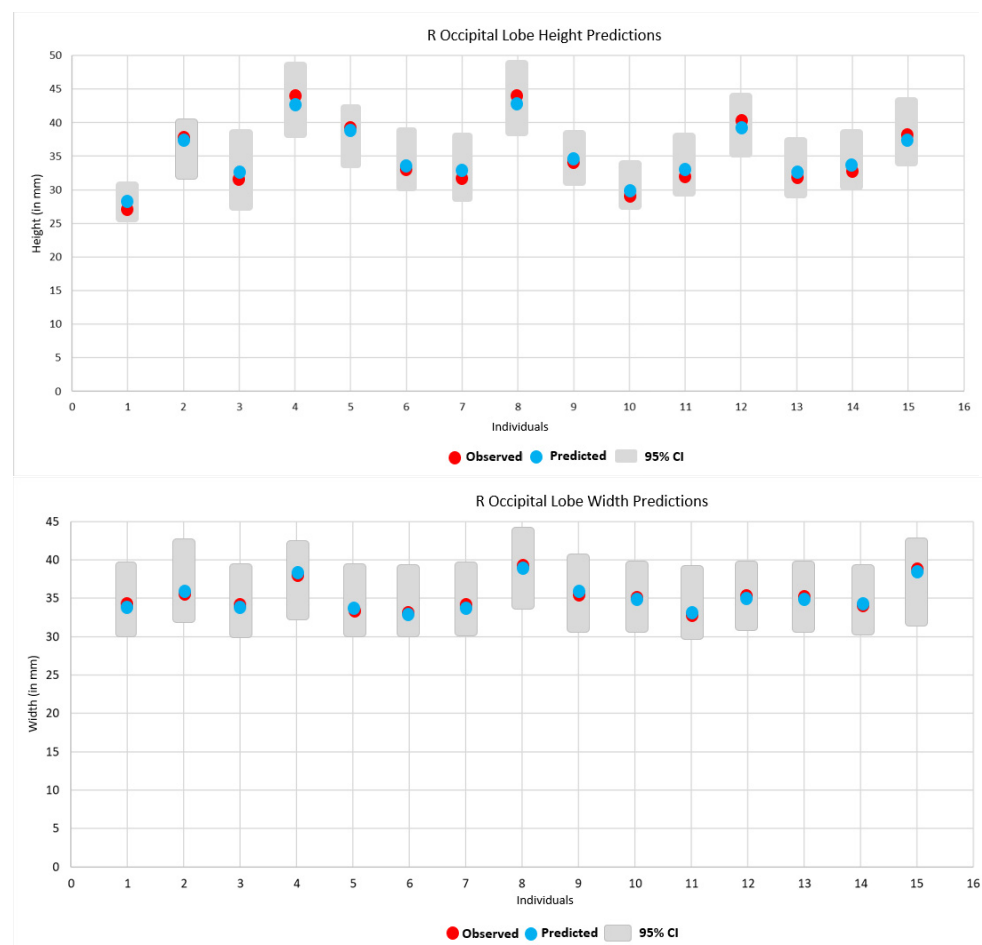


Figure 4. The predicted height and width (in mm) for the R occipital lobe in the known subsample with a confidence interval applied, calculated from the standard error of the regression.

4. Discussion

These findings suggest greater $R > L$ height asymmetry associated with no bridging pattern, moderate $R > L$ height asymmetry for both R and L bridge patterns, smaller $L < R$ height and width asymmetry with a L bridge pattern, and smaller $R < L$ height asymmetry associated with right bridge pattern. Additionally, there was less uncertainty when predicting right and left siding using occipital lobe width rather than occipital lobe height, indicating width is a more reliable predictor than height. This has implications for the suitability of metrics chosen to examine an association with bridging patterns, especially if the sample is unknown where width provides more reliable predictors than height for future research in modelling occipital lobe bridging patterns and possible associations. Although we suggest caution is warranted with the preliminary nature of these results, they also suggest there is a component of asymmetry for chimpanzee occipital lobe bridge patterns, and that increasing width and not simply posterior movement (or reduced height) of the occipital lobe may play an important role in exposure of the occipital-parietal bridge during human evolution, which was unexpected. Future research will compare the size of the parietal to the occipital lobe in these same subjects.

Author Contributions: Conceptualization and methodology, R.H. and S.H.; measurements, G.B.; Statistical analyzes, review and editing, A.P.; original draft preparation, S.H.; review and editing, S.H. All authors have read and agreed to the published version of the manuscript.

Funding: This research received no external funding.

Data Availability Statement: Measurements are contained in the article. MRI data can be obtained from the National Chimpanzee Brain Resource (<https://www.chimpanzeebrain.org> (accessed on 1 September 2021)).

Acknowledgments: The authors would like to thank Chet Sherwood & Aida Gomez-Robles for providing access to the data for these chimpanzees and Antoine Balzeau for inviting us to participate in this Special Issue.

Conflicts of Interest: The authors declare no conflict of interest.

References

1. LeMay, M. Morphological cerebral asymmetries of modern man, fossil man and nonhuman primate. *Ann. N. Y. Acad. Sci.* **1976**, *280*, 349–366. [[CrossRef](#)] [[PubMed](#)]
2. Holloway, R.L.; De La Coste-Lareymondie, M.C. Brain endocast asymmetry in pongids and hominids: Some preliminary findings on the paleontology of cerebral dominance. *Am. J. Phys. Anthropol.* **1982**, *58*, 101–110. [[CrossRef](#)] [[PubMed](#)]
3. Balzeau, A.; Gilissen, E.; Grimaud-Hervé, D. Shared pattern of endocranial shape asymmetries among great apes, anatomically modern humans, and fossil hominins. *PLoS ONE* **2011**, *7*, 29581. [[CrossRef](#)] [[PubMed](#)]
4. Gratiolet, L.P. *Mémoire sur les Plis Cérébraux de L'homme et des Primates*; Bertrand, A., Ed.; Bertrand: Paris, France, 1854.
5. Connolly, J.C. *External Morphology of the Primate Brain*; Thomas, C.C., Ed.; Bannerstone House: Springfield, IL, USA, 1950.
6. Duvernoy, H. *The Human Brain*; Springer: New York, NY, USA, 1991.
7. Holloway, R.L.; Broadfield, D.C.; Yuan, M.S. Morphology and histology of chimpanzee primary visual striate cortex indicate that brain reorganization predated brain expansion in early hominid evolution. *Anat. Rec. A Discov. Mol. Cell Evol. Biol.* **2003**, *273*, 594–602. [[CrossRef](#)] [[PubMed](#)]
8. Falk, D.; Zollikofer, C.P.E.; Ponce de León, M.; Semendeferi, K.; Alatorre Warren, J.L.; Hopkins, W.D. Identification of in vivo Sulci on the External Surface of Eight Adult Chimpanzee Brains: Implications for Interpreting Early Hominin Endocasts. *Brain Behav. Evol.* **2018**, *91*, 45–58. [[CrossRef](#)] [[PubMed](#)]
9. Falk, D. A reanalysis of the South African australopithecine natural endocasts. *Am. J. Phys. Anthropol.* **1980**, *53*, 525–539. [[CrossRef](#)] [[PubMed](#)]
10. Holloway, R. Revisiting the South African Taung australopithecine endocast: The position of the lunate sulcus as determined by the stereoplotting technique. *Am. J. Phys. Anthropol.* **1981**, *56*, 43–58. [[CrossRef](#)]
11. Cointepas, Y.; Mangin, J.F.; Garnero, L.; Poline, J.B.; Benali, H. BrainVISA: Software platform for visualization and analysis of multi-modality brain data. *NeuroImage* **2001**, *13*, 98. [[CrossRef](#)]
12. Gomez-Robles, A.; Hopkins, W.D.; Sherwood, C.C. Increased morphological asymmetry, evolvability and plasticity in human brain evolution. *Proc. R Soc. B* **2013**, *280*, 20130575. [[CrossRef](#)] [[PubMed](#)]
13. Cignoni, P.; Callieri, M.; Corsini, M.; Dellepiane, M.; Ganovelli, F.; Ranzuglia, G. MeshLab: An Open-Source Mesh Processing Tool. In Proceedings of the Sixth Eurographics Italian Chapter Conference, Salerno, Italy, 2–4 July 2008; pp. 129–136.
14. Bailey, R.C.; Byrnes, J. A new, old method for assessing measurement error in both univariate and multivariate morphometric studies. *Syst. Zool.* **1990**, *39*, 124–130. [[CrossRef](#)]
15. Legendre, P.; Legendre, L. *Numerical Ecology*, 3rd ed.; Elsevier: Oxford, UK, 2012; Volume 24.
16. Pearson, A.; Polly, P.D.; Bruner, E. Making sense of modern human sulcal pattern variation, brain size and temporal lobe boundaries: Implications for fossil Homo. *Am. J. Phys. Anthropol.* **2021**, *174*, 83.
17. Press, W.H.; Teukolsky, S.A.; Vetterling, W.T.; Flannery, B.P. *Numerical Recipes in C*; Cambridge University Press: Cambridge, UK, 1992.
18. Simpson, G.G.; Roe, A.; Lewontin, R.C. *Quantitative Zoology*, Rev. ed.; Dover Publications: New York, NY, USA, 2003.
19. Smith, R.J. Allometric scaling in comparative biology: Problems of concept and method. *Am. J. Phys. Anthropol.* **1984**, *246 Pt 2*, R152–R160. [[CrossRef](#)] [[PubMed](#)]
20. Pearson, A.; Polly, P.D.; Bruner, E. Is the middle cranial fossa a reliable predictor of temporal lobe volume in extant and fossil anthropoids? *Am. J. Phys. Anthropol.* **2020**, *172*, 698–713. [[CrossRef](#)] [[PubMed](#)]
21. Hammer, Ø.; Harper, D.A.T.; Ryan, P.D. PAST: Paleontological Statistics Software Package for Education and Data Analysis. *Palaeontol. Electron.* **2001**, *4*, 9.